



n-Butane Dehydrogenation Reaction On Ptxsnyht Catalysts: Effect Of Support On Olefin Selectivity

Shanigaram Prakash¹, Annumandla Ramesh¹, Veldurthi Shashikala^{1,2*}

Student, Student, Assistant Professor

1 – Department of chemistry, University College for Women, Osmania University, Hyderabad, Telangana, India

ABSTRACT:

n – Butane is a natural gas with less reactivity and n-olefins are industrially very important starting materials for the synthesis of fine chemicals. Thus dehydrogenation of n – butane to n-butenes is industrially an important reaction. As this reaction is heterogeneous catalytic reactions are carried out at high temperature results in various products were obtained with cracking, dehydrogenation, isomerization and polymerization reactions. Among all dehydrogen products are industrially very important. In present work we have studied the effect of calcined hydrotalcite supports on the activity of Pt and PtSn catalysts for this reaction. A series of three catalysts of PtyHT and another series of three catalysts Pt03SnyHT were prepared by impregnation method. All the catalysts were dried, calcined and reduced before studying their properties and testing their activity. Phase of these catalysts was identified from XRD. Specific surface area was obtained from BET method. Distribution of the particles and their sizes were obtained from TEM and CO chemisorption studies. N-Butane dehydrogenation reaction was performed by passing n-butane : H₂ : N₂ feed flow rate 30 ml/min on 100 mg catalyst placed in a fixed bed SS reactor. Reaction temperature was maintained at 500 °C.

Index Terms – n- butane, dehydrogenation, PtxSnyHT, basicity, Olefin selectivity

1. Introduction:

Synthesis of light olefins from dehydrogenation of lower alkanes (C₁–C₄) is an industrially important reaction. n-Butane dehydrogenation has been studied on PtSn catalysts supported on Al₂O₃ and ZnAl₂O₄ [1–3]. Various undesired reactions such as cracking, isomerization and polymerization were intensified with an increase in the acidity of the supports [4–6]. Thus, an attempt was made to select the supports with the base property such as alkali earth metal oxides to reduce the side reactions. MgO with Lewis and Brönsted (O²⁻ and OH⁻) basic sites has been considered as an important solid base catalyst for many organic transformations in heterogeneous catalysis [7, 8], which has been used as supports to disperse active metal components such as Pt, Pd, Rh, and Ni [9–15]. However, the inherent properties of MgO such as dissolution and reprecipitation in an aqueous solution and the strong metal support interactions limited its applications to heterogeneous catalysis [9, 15–18]. In the process of the catalyst preparation using MgO support, it was observed that the active metal particles could be encapsulated by the support [16, 17]. The strong metal support interactions and formation of Pt–MgO complex were also reported [9, 18]. To overcome the disadvantages of MgO support Veldurthi Shashikala et al has reported n-Butane dehydrogenation on Pt-Sn supported on carbon modified MgO catalysts [19]. The modification of magnesium oxide with carbon (CMgO) increased the covalent character of the Mg–O bond. Hydrotalcite are important materials which showed various applications as an adsorbent, supports for

various catalysts [20]. Calcined hydrotalcites of Al_2O_3 and MgO has both the properties of alumina (high surface area) and magnesia (basicity) [21]. Platinum nano particles dispersed on various supports showed their best dehydrogenation activity, and tin was being act as promoter by modifying the chemical environment of the platinum to reduce the cracking products [1-3, 9 22,23]. Thus in the present work we have studied the affect of support on conversion of n-butane to n-butenes (i.e. n-butene selectivity) with an active catalyst Pt catalyst with 1 weight percent. And also the promotional effect of Sn was also studied with a standardized 0.3 weight percentage of tin [19].

Experimental:

2.1 Preparation of catalysts

A series of three adsorbents with mole ratios of magnesium oxide to alumina with 1 : 1 (1HT), 1 : 2 (2HT), 1 : 3 (3HT) were synthesizes by standard co-precipitation method under super saturation conditions, this synthesis procedure was given in detail in our previous report [24]. According to the procedure given by Shanigaram Prakash et al metal nitrates of alumina and magnesia were taken as precursors. Corresponding weights of magnesium nitrate and aluminium nitrate salts were dissolved distilled water to make 10% solution. This salt mixture was thoroughly stirred with a mechanical stirrer to prepare a homogenous solution. Ten percent each of sodium hydroxide and sodium carbonate solutions, hydroxide and carbonate are the common interlayer anionic species, were taken in two different separating flasks and added these solutions simultaneously. Very slow and continuous addition with stirring was done, at pH 9 a thick viscous precipitate was formed stirring and addition of the precipitating agents was continued until the pH reaches to 11. Addition of these precipitating agents was performed at room temperature and after completion of the addition the temperature of the precipitant was increased to 333-338 K was kept for aging in hydrothermal conditions [25] for 18 hrs. This gel lie precipitant was then cooled to room temperature followed by filtration. Thus obtained white cake was washed with distilled water till the filtrate shows pH of 7. Then this cake was oven dried at 393 K for overnight and calcined at 723 K for 18 h.

After calcinations these materials were named as 1HT, 2HT and 3HT. A series of six catalysts in two sets were prepared. Among these two sets one was dispersion of 1 weight percentage of platinum and another set was with 1 weight percent platinum and 0.3 weight percent of tin. These active catalysts were dispersed on these three supports by impregnation method[26-28]. Chloride precursors of platinum, tin were purchased from SRL chemicals, India. Corresponding weights of the precursors to yield 1wt% of platinum and 0.3 wt % of tin were impregnated from their aqueous solutions on to the hydrotalcite supports, these catalysts were named as $\text{Pt}_x\text{Sn}_y\text{HT}$ ($x = 0$ and 0.3). After impregnation these catalysts were dried in hot air oven for overnight at 120 °C and then calcined at 500 °C for 5 h. Then each catalyst was reduced in situ under H_2 atmosphere at same temperature for 2 hrs before testing the dehydrogenation activity. Reduction and activity tests were performed at 500 °C.

2.2 Catalyst Characterization:

The Phase identification and conformation of as prepared support materials was done with the help of Rigaku XRD 6000 diffractometer with Ni filtered $\text{CuK}\alpha$ radiation at 40 kV, 30 mA was used for X-ray diffraction analysis. N_2 -physisorption analysis was carried out on a Micromeritics ASAP 2020 at 196 °C. The specific surface areas of the dried and calcined hydrotalcites and reduced $1\text{Pt}0.3\text{Sn}_y\text{HT}$ samples were obtained using the BET and BJH equations, respectively. BELCAT catalyst analyzer was used to study the metal dispersion by CO chemisorptions studies. Transmission electron microscopic technique on Analytical Transmission Electron Microscope (model – CM30 TEM, Philips) with an accelerating voltage 200 kV was used to get the high resolution images.

2.3 Activity Evaluation:

To study the n-butane dehydrogenation activity of these $1\text{Pt}_x\text{Sn}_y\text{HT}$ catalysts, 100 mg of calcined catalyst was loaded in a fixed bed SS tubular reactor at reaction temperature 500 °C, with a feed flow rate 30 ml/min. Before performing the reaction all the catalysts were reduced in-situ using H_2 gas at 50 ml/min of flow rate for 2 hrs. The products generated in the reaction were analyzed using an on-line gas chromatography with

Al₂O₃/KCl capillary column (I.D.: 0.53 mm, length: 50 m, Agilent Technologies). Selectivity of the products and stability of the catalysts for reactant conversion was studied with time on stream studies for 5 hrs.

3. Results and discussion

3.1 X – ray diffraction:

X ray diffraction patterns of reduced catalysts after impregnation of platinum and platinum-tin on 1HT, 2HT, and 3HT were presented in figure 1 and 2 respectively. On close observation of both the diffractogram patterns, the hydrotalcite phase was reappeared. As stated from our previous paper that, the XRD patterns of the dried samples match with the ICDD file number 890460 with sharp and symmetric peaks for (003), (006), (110), and (113) planes at 2 theta scale 11.65, 23.42, 60.95 and 62.46 respectively as well as broad symmetric peaks for the (009), (015), and (018) planes at 2 theta scale of 34.90, 39.85 and 47.59 respectively. These peaks are characteristics of clay minerals having layered structures [29-31]. And also it was seen from the dried supports XRD of the previous paper a perfect LDH crystal structure was present with 2HT and 3HT where the Al₂O₃:MgO mole ratio is 1:2 and 1:3 respectively [24]. The formation of little of the hydrotalcite phase in platinum impregnated catalysts may be due to the memory effect of the LDH materials [32]. However separation of magnesia (ICDD – 87-0651) and alumina (ICDD 04-0875) phases were also observed in figure 1 that is for platinum impregnated catalysts. For platinum tin loaded hydrotalcite catalysts, the phase hydrotalcite was more prominent compare to platinum loaded supports. This might be due to incorporation of sufficient number of interlayer anions, i.e. Cl⁻ from the metal precursors and water molecules from aqueous solution, in the process of impregnation and this phase might be more thermal stable that this hydrotalcite phase exists even after reduction. And the intensity of alumina peaks was decreased from P03Sn1HT to P03Sn3HT. Less intense broad peaks of hydrotalcites in P03Sn3HT might be due to the formation of small crystallites. However in PtSn loaded catalysts after reduction, MgO phase could not be separated.

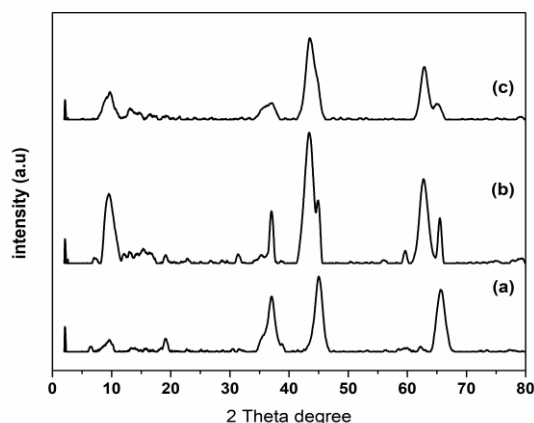


Figure 1: X ray diffraction patterns of reduced catalysts after impregnation of platinum on a)Pt1HT ,b)Pt2HT,c)Pt3HT

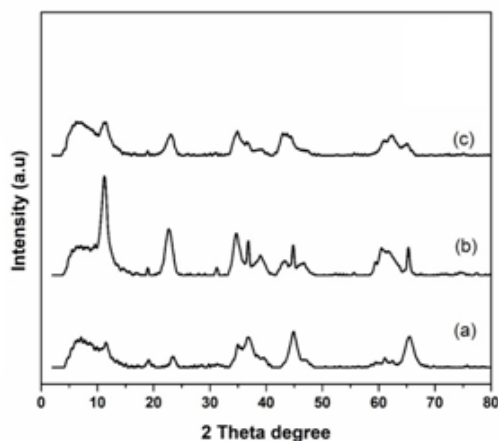


Figure 2: X ray diffraction patterns of reduced catalysts after impregnation of platinum-tin on a)Pt03Sn1HT,b)Pt03Sn2HT, c)Pt03Sn3HT

3.2 BET surface area:

Specific surface areas of the supports after calcination, (yHT) and the active catalysts PtyHT and PtxSnyHT after reduction were obtained using BET method and the values were given in table 1. In calcined hydrotalcites the surface area is increased from 1HT to 3HT which was already explained in previous paper [24]. There observed large decrease in the reduced catalysts of platinum, platinum – tin loaded yHT. This might be due to change in the phase of the support material with impregnation and dispersion of active catalyst in the pores. There observed decreasing order of surface areas of supports, monometallic catalysts PtyHT, and bimetallic catalysts PtxSnyHT. This can be understood from the XRD patterns of these catalysts. There observed many phases in bimetallic catalysts than in monometallic catalysts. In the process of separation of phases the smaller particles might block the specific surface area of the catalysts.

Table 1: Specific surface area of supports yHT, active catalysts PtxSnyHT

Samp le	BET SA (m ² /g)	Sample	BET SA (m ² /g)	Sample	BET SA (m ² /g)
1HT	235	Pt1HT	146	Pt03Sn1HT	138
2HT	254	Pt2HT	141	Pt03Sn2HT	104
3HT	278	Pt3HT	121	Pt03Sn3HT	92

3.3 Transmission Electron Microscopy:

Transmission electron micrographs of monometallic catalysts (PtyHT) and bimetallic catalysts (Pt03SnyHT) were presented in figure 3. High resolution images of platinum dispersed on hydrotalcite materials were presented at the first row of the figure 3, image 3A was of Pt1HT, 3B was of Pt2HT and 3C was of Pt3HT. Where in the particles size of platinum obtained were below 5 nm size. The nature of dispersion of the platinum metal was almost same on all the three supports. It was observed that fine dispersion with narrow size distribution was observed on all the supports. Second row of images were of bimetallic catalysts dispersed on hydrotalcite supports, image 3-1 was for Pt03Sn on 1HT, 3-2 for 2HT, and 3-3 was dispersion on 3HT supports. The bimetallic catalysts also showed fine dispersion with narrow size distribution. With change in the mole percentages of alumina and magnesia there observed change in crystal phases. However, there could not observe any major difference in the morphological dispersion of the monometal or bimetal catalysts distribution on supports with different phases. In a an article published by S. Veldurthi et al platinum dispersion of pure magnesium oxide showed bimodal particle size disteibution. This kind of bimodal distribution was also observed by Tanabe T et al and Rickard JM et al too. As explained by them this might be due to the migration and sintering of metal particles (see the HRTEM image of Pt/MgO) present at the lattice boundaries of MgO [19, 9, 26]. Though we observe MgO phase in calcine 2HT and 3HT supports in the Pt2HT

and Pt3HT catalysts bimodal distribution was not observed. In these calcined hydrotalcite supports though the phase of MgO was observed in XRD, there is difference in the chemical properties of the MgO present along with alumina, MgAlO₄ spinel etc support. Thus there was not observed any sintering dissolution properties found.

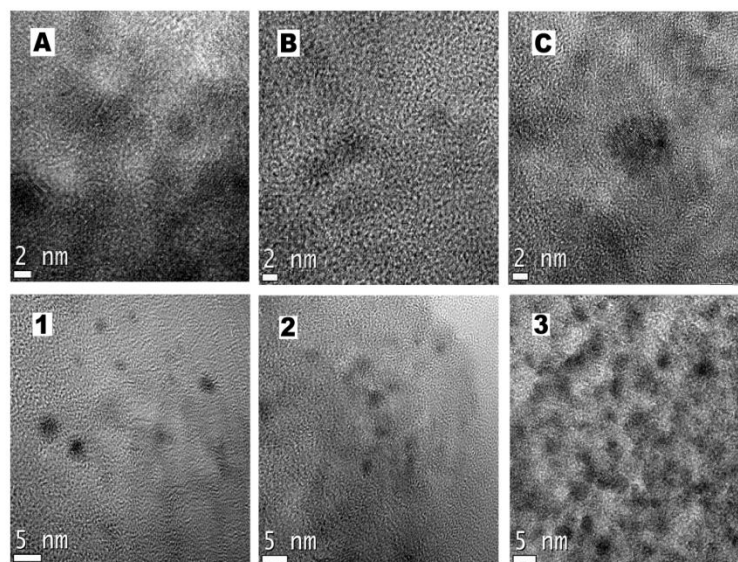


Figure 3: Transmission electron micrographs of platinum (1st row), platinum and tin (2nd row) dispersed yHT supports, images were obtained after reduction.

A – Pt1HT, B – Pt2HT, C – Pt3HT and
1 – Pt0.3Sn1HT, 2 - Pt0.3Sn2HT and 3 – Pt0.3Sn3HT

3.4 Metal dispersion, metal surface area, particle size by CO chemisorption

In the case of metal catalysts dispersed on a support, the catalytically active component of supported catalyst was often concentrated in a separate phase distinguishable from inactive phase. This active catalyst dispersion can be calculated by the chemisorption of various small molecules like CO, H₂ or O₂ etc for different metals. In this study we have used 5% CO in He gas molecules to adsorb on Pt, PtSn active catalysts.

CO pulse chemisorption was performed to acquire average particle sizes, metal surface areas and distributions of metal particles. Before measuring the pulse chemisorptions, all the catalysts were pretreated as follows. A total of 50 mg of the prereduced (with H₂ gas flow rate 30 mL/min, 500 °C for 2 h) catalyst was placed in the U type quartz reactor connected to the BELCAT catalyst analyzer. Initially, the catalyst surface was purged for 1 h with He gas flow (flow rate 50 mL/min) at 400 °C. Then, the catalysts were re-reduced followed by purging with He gas at the same temperature for 30 min to remove the excess H₂ adsorbed on the catalysts surface. The reactor was permitted to cool till 40 °C. At this temperature, the 5% CO in He gas adsorbed in pulses until no further adsorption of CO occurred. The metal dispersion was calculated from the amount of CO gas adsorbed on the catalysts considering the stoichiometry factor as one.

$$\text{Metal dispersion} = \frac{V \times 22,414 \times SF \times MW}{C} \times 100$$

Where, V was the amount of carbon monoxide adsorbed (mL), MW was the atomic weight of metal (g. mol⁻¹), SF was the stoichiometry factor, and C was the weight of the supported metal on the sample (g).

Table 2: Percentage dispersion of metal, metal surface area, and particle size of the Pt, PtSn active metal on impregnation of Pt and PtSn on yHT obtained from CO chemisorptions studies.

Catalysts	Metal dispersion (%)	Metal surface area (m ² /g)	Particle diameter (nm)
Pt1HT	15.87	0.39	7.14

Pt2HT	51.91	1.28	2.82
Pt3HT	50.77	1.25	2.23
Pt03Sn1HT	57.34	1.42	1.97
Pt03Sn2HT	53.25	1.30	2.12
Pt03Sn3HT	51.22	1.26	2.21

3.5 Activity of mono metallic catalyst:

Activity of mono metallic catalyst was studied by passing n-butane:H₂:N₂ gasses (feed stock) with equal volume ratio a total flow rate of 30 ml/min at atmospheric pressure with 500 °C temperature. The flow rate was controlled by mass flow controllers. All the catalysts show high activity in the range from 30 – 38 % at the initial minutes. However the activity of Pt1HT is decreased rapidly, this might be due to high cracking products and carbon deposition on Pt1HT. This percentage conversion on monometallic catalysts was in relation with the metal dispersion obtained from CO chemisorptions. Thus this reduction in the conversion with time might also be due to decrease in the availability of the suitable active sites for n – butane dehydrogenation. Selectivity for n-butenes is in-line with the conversion i.e. high conversion less selectivity and vice versa. The activity of mono metallic catalyst was studied for 5 hrs. Time on stream stream study data i.e. percentage conversion and selectivity were given as pictorial representation in figure 4.

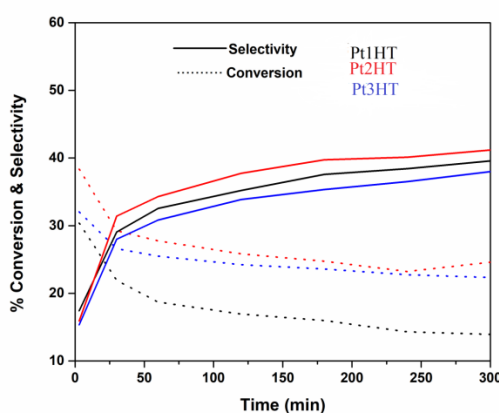


Figure 4: Activity of mono metallic catalyst percentage conversion and selectivity

3.6 Activity of bimetallic catalyst:

Activity of bimetallic catalyst was also studied with same conditions as like monodispersed catalysts i.e. by passing n-butane:H₂:N₂ gasses (feed stock) with equal volume ratio a total flow rate of 30 ml/min at atmospheric pressure with 500 °C temperature. The flow rate was controlled by mass flow controllers. With addition of tin to the platinum increased the percentage conversion from 30-38 to 63-72 and the selectivity was increased upto 67 percent. All the catalysts show high activity in the 3 minute and there showed almost same conversion for all the catalysts i.e. PtSn catalysts dispersed on three different hydrotalcite supports. This can be explained from the metal dispersion values obtained from both CO chemisorptions and TEM analysis. However there is change in the n – butane selectivities on the three catalysts. Selectivity of n – butane is increased with increase in the MgO ratio. The activity of bimetallic catalyst was studied for 5 hrs. Time on stream stream study data i.e. percentage conversion and selectivity were given as pictorial representation in figure 5. Among all six catalysts PtSn3HT showed good activity with high selectivity.

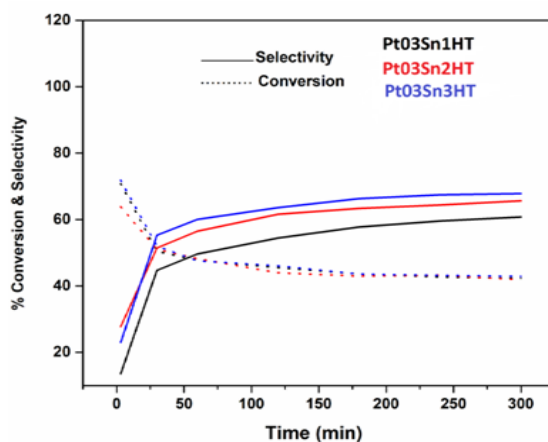


Figure 5: Activity of bimetallic catalyst percentage conversion and selectivity

4. Conclusion:

Present work focused on the support effect of calcined hydrotalcites on dehydrogenation reaction. Active catalyst platinum supporting on calcined hydrotalcites and active catalyst platinum and promoter tin were supported on calcined hydrotalcites. Phase and surface area of the reduced catalysts were obtained with the help of XRD and N_2 adsorption studies respectively. Platinum and platinum – tin particles size and distribution were obtained with the help of transmission electron microscopy and CO chemisorption studies. Butane dehydrogenation activity of just platinum impregnated calcined hydrotalcite catalysts can be explained from the CO chemisorptions results. On the addition of promoters tin to the platinum i.e. PtSn impregnated on calcined hydrotalcites, dehydrogenation activity of the all the catalysts was observed same. And the selectivity to n-butenes is increased with increase in basicity of the support.

Acknowledgements:

Authors acknowledge Osmania University and Veeranari Chakali Iilamma University for providing facilities to complete the research work.

Reference:

1. Nijhuis, T. A., Kreutzer, M. T., Romijn, A. C. J., Kapteijn, F., & Moulijn, J. A. (2001). Monolithic catalysts as efficient three-phase reactors. *Chemical Engineering Science*, 56(3), 823-829. [https://doi.org/10.1016/S0009-2509\(00\)00294-3](https://doi.org/10.1016/S0009-2509(00)00294-3)
2. Meille, V. (2006). Review on methods to deposit catalysts on structured surfaces. *Applied Catalysis A: General*, 315, 1-17. <https://doi.org/10.1016/j.apcata.2006.08.031>
3. Cristiani, C., Visconti, C. G., Finocchio, E., Stampino, P. G., & Forzatti, P. (2009). Towards the rationalization of the washcoating process conditions. *Catalysis Today*, 147, S24-S29. <https://doi.org/10.1016/j.cattod.2009.07.031>
4. Wojciechowski, B. W., & Corma, A. (1986). Catalytic cracking: catalysts, chemistry, and kinetics.
5. Venuto, P. B. (1994). Organic catalysis over zeolites: a perspective on reaction paths within micropores. *Microporous Materials*, 2(5), 297-411. [https://doi.org/10.1016/0927-6513\(94\)00002-6](https://doi.org/10.1016/0927-6513(94)00002-6)
6. Bekkum, H. V. (1988). Kouwenhoven, stud. *Surf Sci. Catal*, 41, 45.
7. Julkapli, N. M., & Bagheri, S. (2016). Magnesium oxide as a heterogeneous catalyst support. *Reviews in Inorganic Chemistry*, 36(1), 1-41. <http://doi.org/10.1515/revic-2015-0010>
8. Bailly, M. L., Chizallet, C., Costentin, G., Krafft, J. M., Laumon-Pernot, H., & Che, M. (2005). A spectroscopy and catalysis study of the nature of active sites of MgO catalysts: Thermodynamic Brønsted basicity versus reactivity of basic sites. *Journal of Catalysis*, 235(2), 413-422. <https://doi.org/10.1016/j.jcat.2005.09.004>
9. Flytzani-Stephanopoulos, M., & Gates, B. C. (2012). Atomically dispersed supported metal catalysts. *Annual review of chemical and biomolecular engineering*, 3(1), 545-574. <https://doi.org/10.1146/annurev-chembioeng-062011-080939>

10. Sui, X., Zhang, L., Li, J., Doyle-Davis, K., Li, R., Wang, Z., & Sun, X. (2022). Advanced support materials and interactions for atomically dispersed noble-metal catalysts: from support effects to design strategies. *Advanced Energy Materials*, 12(1), 2102556. <https://doi.org/10.1002/aenm.202102556>
11. Mehrabadi, B. A., Eskandari, S., Khan, U., White, R. D., & Regalbuto, J. R. (2017). A review of preparation methods for supported metal catalysts. *Advances in catalysis*, 61, 1-35. <https://doi.org/10.1016/bs.acat.2017.10.001>
12. Ruckenstein, E., & Dadyburjor, D. B. (1983). Sintering and redispersion in supported metal catalysts. *Reviews in Chemical Engineering*, 1(3), 251-356.
13. Gates, B. C., Flytzani-Stephanopoulos, M., Dixon, D. A., & Katz, A. (2017). Atomically dispersed supported metal catalysts: perspectives and suggestions for future research. *Catalysis Science & Technology*, 7(19), 4259-4275. <https://doi.org/10.1039/C7CY00881C>
14. Boudart, M. (1969). Catalysis by supported metals. *Advances in catalysis*, 20, 153-166. [https://doi.org/10.1016/S0360-0564\(08\)60271-0](https://doi.org/10.1016/S0360-0564(08)60271-0).
15. Tauster, S. J. (1987). Strong metal-support interactions. *Accounts of Chemical Research*, 20(11), 389-394. <https://doi.org/10.1002/smt.201700286>.
16. Julkapli, N. M., & Bagheri, S. (2016). Magnesium oxide as a heterogeneous catalyst support. *Reviews in Inorganic Chemistry*, 36(1), 1-41. <https://doi.org/10.1515/revic-2015-0010>.
17. De Rogatis, L., Cargnello, M., Gombac, V., Lorenzut, B., Montini, T., & Fornasiero, P. (2010). Embedded phases: a way to active and stable catalysts. *ChemSusChem: Chemistry & Sustainability Energy & Materials*, 3(1), 24-42. <https://doi.org/10.1002/cssc.200900151>
18. Gao, C., Lyu, F., & Yin, Y. (2020). Encapsulated metal nanoparticles for catalysis. *Chemical Reviews*, 121(2), 834-881.
19. Shashikala, V., Jung, H., Shin, C. H., Koh, H. L., & Jung, K. D. (2013). N-butane dehydrogenation on PtSn/carbon modified MgO catalysts. *Catalysis letters*, 143(7), 651-656. DOI 10.1007/s10562-013-1009-3
20. Ballarini, A. D., Zgolicz, P., Vilella, I. M., de Miguel, S. R., Castro, A. A., & Scelza, O. A. (2010). n-Butane dehydrogenation on Pt, PtSn and PtGe supported on γ -Al₂O₃ deposited on spheres of α -Al₂O₃ by washcoating. *Applied Catalysis A: General*, 381(1-2), 83-91. <https://doi.org/10.1016/j.apcata.2010.03.053>
21. Vaccari, A., & Gazzano, M. (1995). Hydrotalcite-type anionic clays as precursors of high-surface-area Ni/Mg/Al mixed oxides. In *Studies in Surface Science and Catalysis* (Vol. 91, pp. 893-902). Elsevier. [https://doi.org/10.1016/S0167-2991\(06\)81832-X](https://doi.org/10.1016/S0167-2991(06)81832-X)
22. Tian, L., Chen, Y., Wu, S., Cai, Y., Liu, H., Zhang, J., ... & Cheng, Y. (2017). One-pot synthesis of cubic PtPdCu nanocages with enhanced electrocatalytic activity for reduction of H₂O₂. *RSC Advances*, 7(54), 34071-34076. DOI: 10.1039/C7RA03220J
23. Wang, P., Chae, S., Deng, Z., Liu, Y., Zhu, Z., Sawada, Y., & Saito, N. (2025). Highly Dispersed PtPdCu Nanoparticles for Oxygen Reduction Catalytic Performance and Electronic State. *The Journal of Physical Chemistry C*, 129(20),
24. Shanigaram Prakash, Annumandla Ramesh, Erugu Bhoomika, Veldurthi Shashikala, "Calcined Hydrotalcite materials as Efficient Adsorbents for CO₂ and N₂O Gases", IJRAR - International Journal of Research and Analytical Reviews (IJRAR), E-ISSN 2348-1269, P- ISSN 2349-5138, Volume.12, Issue 3, Page No pp.855-867, July 2025, <https://doi.org/10.56975/ijrar.v12i3.317364>
25. Roy, R., & Tuttle, O. F. (1956). Investigations under hydrothermal conditions. *Physics and Chemistry of the Earth*, 1, 138-180. [https://doi.org/10.1016/0079-1946\(56\)90008-8](https://doi.org/10.1016/0079-1946(56)90008-8)
26. Girish, C. R. (2018). Various impregnation methods used for the surface modification of the adsorbent: A review. *Int. J. Eng. Technol*, 7(4.7), 330-334.
27. Shimokawabe, M., Asakawa, H., & Takezawa, N. (1990). Characterization of copper/zirconia catalysts prepared by an impregnation method. *Applied Catalysis*, 59(1), 45-58. [https://doi.org/10.1016/S0166-9834\(00\)82186-7](https://doi.org/10.1016/S0166-9834(00)82186-7)
28. Lee, S. Y., & Aris, R. (1985). The distribution of active ingredients in supported catalysts prepared by impregnation. *Catalysis Reviews Science and Engineering*, 27(2), 207-340. <https://doi.org/10.1080/01614948508064737>
29. Kumari, N., & Mohan, C. (2021). Basics of clay minerals and their characteristic properties. *Clay Clay Miner*, 24(1), 1-29.

30. Hendricks, S. B. (1942). Lattice structure of clay minerals and some properties of clays. *The Journal of geology*, 50(3), 276-290. <https://doi.org/10.1086/625051>.
31. Drits, V. A. (2003). Structural and chemical heterogeneity of layer silicates and clay minerals. *Clay Minerals*, 38(4), 403-432. <https://doi.org/10.1180/0009855033840106>
32. Benito, P., Fornasari, G., Basile, F., Tabanelli, T., Lucarelli, C., Fasolini, A., ... & Trifiro, F. (2024). The several hydrotalcites investigated as precursors of catalysts by Angelo Vaccari. *Catalysis Today*, 439, 114791. <https://doi.org/10.1016/j.cattod.2024.114791>

